© 2022. Published by The Company of Biologists Ltd | Journal of Cell Science (2022) 135, jcs259617. doi:10.1242/jcs.259617

RESEARCH ARTICLE

VEGF-A controls the expression of its regulator of angiogenic functions, dopamine D2 receptor, on endothelial cells

Chandrani Sarkar[1,2,3,4,5,*], Debanjan Chakroborty[1,2,3,4,5,*], Sandeep Goswami[1,3,4,*], Hao Fan[1], Xiaokui Mo[6] and Sujit Basu[1,2,7,‡]

ABSTRACT

We have previously demonstrated significant upregulation of dopamine D2 (DAD2) receptor (DRD2) expression on tumor endothelial cells. The dopamine D2 receptors, upon activation, inhibit the proangiogenic actions of vascular endothelial growth factor-A (VEGF-A, also known as vascular permeability factor). Interestingly, unlike tumor endothelial cells, normal endothelial cells exhibit very low to no expression of dopamine D2 receptors. Here, for the first time, we demonstrate that through paracrine signaling, VEGF-A can control the expression of dopamine D2 receptors on endothelial cells via Krüppel-like factor 11 (KLF11)-extracellular signal-regulated kinase (ERK) 1/2 pathway. These results thus reveal a novel bidirectional communication between VEGF-A and DAD2 receptors.

KEY WORDS: VEGF-A, Dopamine D2 receptor, Endothelial cell

INTRODUCTION

Vascular permeability factor or vascular endothelial growth factor-A (VEGF-A), a potent cytokine, and dopamine (DA), an important neurotransmitter/neurohormone, play essential roles in many critical physiological and pathological settings (Folkman, 2004; Dvorak, 2005; Apte et al., 2019; Missale et al., 1998; Rubí and Maechler, 2010; Beaulieu et al., 2015; Franco et al., 2021). DA has been previously shown to modulate the process of VEGF-A-induced angiogenesis in different disorders (Basu et al., 2001; Chakroborty et al., 2004, 2016; Chauvet et al., 2017; Tejada et al., 2021). Whereas VEGF-A stimulates angiogenesis mainly by acting through vascular endothelial growth factor receptor-2 (VEGFR-2; also known as KDR), the regulatory effect of DA on VEGF-A mediated actions on endothelial cells (ECs) largely depends upon the expression of specific classes of DA receptors on these cells (Folkman, 2004; Dvorak, 2005; Apte et al., 2019; Basu et al., 2001; Chakroborty et al., 2016).

We had previously demonstrated that loss of DA D2 (DAD2) receptor (symbol DRD2) receptors in endothelial cells (ECs) and endothelial progenitor cells enhances VEGF-A-induced angiogenesis (Basu et al., 2004; Chakroborty et al., 2008). Furthermore, DA acting through its D2 receptors expressed on ECs can also inhibit VEGF-A-induced angiogenesis (Basu et al., 2001; Chakroborty et al., 2004; Chauvet et al., 2017; Tejada et al., 2021). However, the status of DAD2 receptor expression differs significantly between normal and tumor endothelial cells (TECs) (Basu et al., 2001; Chakroborty et al., 2004, 2011). Normal ECs have a very low or no surface expression of DAD2 receptors, which, in contrast, is considerably upregulated in TECs (Basu et al., 2001; Chakroborty et al., 2004, 2011).

Although the antagonism between the stimulation of DAD2 receptors and VEGF-A mediated angiogenic functions is well known (Basu et al., 2001; Chakroborty et al., 2004; Chauvet et al., 2017; Tejada et al., 2021), there is no information regarding the factors that regulate DAD2 receptor expression on TECs. Using different VEGF-A producing tumor models, a VEGF-A knockdown tumor model and a stringent model of VEGF-A-induced angiogenesis, we here, for the first time, report that VEGF-A is a crucial regulator of DAD2 receptor expression on ECs, which in turn upon activation can modulate VEGF-A-induced angiogenesis. Therefore, this study establishes a new and novel feedback loop between VEGF-A-induced angiogenesis and the expression of DAD2 receptors on ECs.

RESULTS

Effect of VEGF-A on DAD2 receptor expression on endothelial cells

Since high expression of DAD2 receptors is observed on TECs and because malignant tumor cells produce a significant amount of VEGF-A (Jayson et al., 2012), initial experiments were performed to determine whether VEGF-A secreted by tumor cells has any role in the expression of DAD2 receptors on TECs. *In vivo* experiments were performed using well-characterized orthotopic HT29 human colon cancer cells (HT29+VEGF-A$^{+/+}$ cells) and an orthotopic HT29 human colon cancer model developed from HT29 cells in which the VEGF-A gene was knocked down by CRISPR/Cas9 gene editing (HT29+VEGF-A$^{-/-}$ cells) (Figs S1 and S2), thereby reducing the primary source of VEGF-A in the tumor microenvironment. Knockdown of VEGF-A in HT29 cells was confirmed by real-time quantitative PCR (qPCR) and enzyme-linked immunosorbent assay (ELISA) of the culture supernatant (Fig. 1A,B). After orthotopic implantation of tumor cells into nude mice, considerably high expression of DAD2 receptors on the TECs was observed in HT29+VEGF-A$^{+/+}$ tumors compared to ECs in normal colon tissues (Fig. 1C). However, unlike in the TECs of HT29+VEGF-A$^{+/+}$ tumors, upregulation of DAD2 receptors was not observed on the TECs of mice transplanted with HT29+VEGF-A$^{-/-}$ human colon cancer cells (Fig. 1C) (P<0.05).

A similarly high expression of DAD2 receptors was demonstrated on the TECs of VEGF-A-secreting well-differentiated human colon

[1]Department of Pathology, Ohio State University, Columbus, Ohio 43201, USA. [2]Comprehensive Cancer Center, Ohio State University, Columbus, Ohio 43210, USA. [3]Department of Pathology, University of South Alabama, Mobile, Alabama 36617, USA. [4]Cancer Biology Program, Mitchell Cancer Institute, University of South Alabama, Mobile, Alabama 36688, USA. [5]Department of Biochemistry & Molecular Biology, University of South Alabama, Mobile, Alabama 36688, USA. [6]Department of Biomedical Informatics, Ohio State University, Columbus, Ohio 43210, USA. [7]Division of Medical Oncology, Department of Internal Medicine, Ohio State University, Columbus, Ohio 43210, USA.
*These authors contributed equally to this work

‡Author for correspondence (Sujit.Basu@osumc.edu)

H.F., 0000-0003-4797-7954; S.B., 0000-0002-8272-0807

Handling Editor: John Heath
Received 22 November 2021; Accepted 5 May 2022

Journal of Cell Science (2022) 135, jcs259617. doi:10.1242/jcs.259617

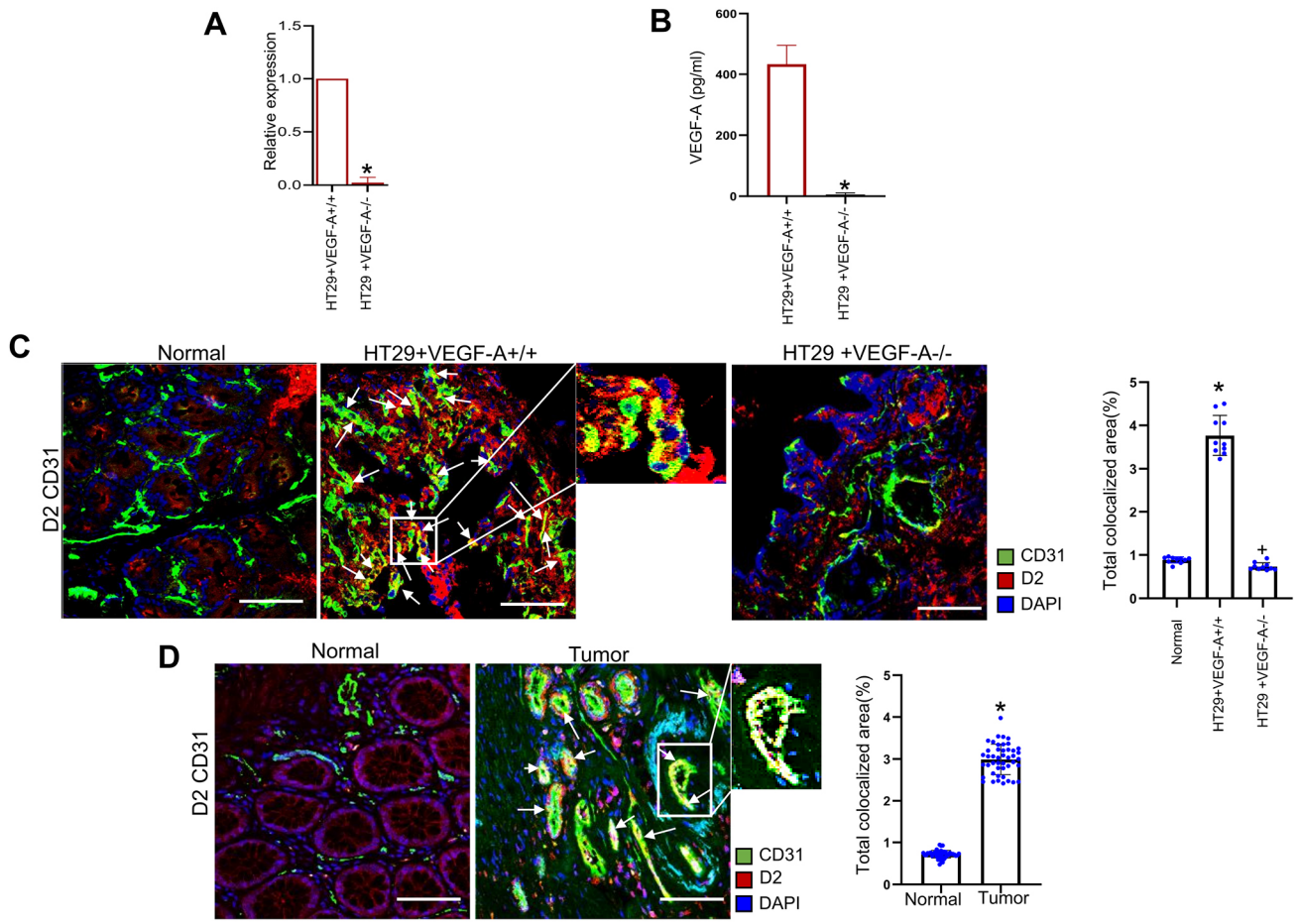

Fig. 1. VEGF-A affects DAD2 receptor expression in endothelial cells. Knockdown of VEGF-A in HT29 cells was confirmed by (A) real-time qPCR and (B) ELISA. Data are expressed as the mean±s.e.m. (n=3). *P<0.05 (two-sample two-tailed t-test). (C) Representative images of colocalization (arrows) of CD31 and DAD2 receptors [i.e. expression of DAD2 receptors on the tumor endothelial cells (TECs)]. TECs (green) of HT29+VEGF-A^{+}/$^{+}$ tumors showed significantly higher expressions of DAD2 receptors (red) compared to TECs of HT29+VEGF-A^{-}/$^{-}$ tumors and endothelial cells (ECs) of normal colon tissues (n=10 for each group). Scale bars: 80 µm. Right, ten fields of view were randomly chosen and analyzed. Data are expressed as the mean±s.e.m. *P<0.05 for HT29+VEGF-A+/+ versus normal; ^{+}P<0.05 for HT29+VEGF-A^{-}/$^{-}$ versus HT29+VEGF-A+/+ (one-way ANOVA with Bonferroni step down adjustment). (D) Representative images of colocalization (arrows) of CD31/dopamine D2 receptors indicate high expressions of DAD2 receptors on TECs of VEGF-A secreting well-differentiated human colon adenocarcinoma tissues compared to the ECs of normal colon tissues (n=45 for each group). Scale bars: 80 µm. Right, four fields of view per section were randomly chosen and analyzed. Data are expressed as the mean±s.e.m. *P<0.05 for tumor versus normal (two-sample two-tailed t-test).

carcinoma tissues. By contrast, there was no or low expression of DAD2 receptors on the ECs of the blood vessels in normal human colon tissues (Fig. 1D; P<0.05). These results suggest that VEGF-A can induce DAD2 receptor expression on TECs.

Next, to determine the specificity of VEGF-A action on the expression of DAD2 receptors, a stringent model of angiogenesis was selected in which an adenoviral (Ad)VEGF-A was engineered to express the murine VEGF-A 164-amino-acid isoform under the control of the cytomegalovirus promoter and was subsequently introduced into the ears of nude mice (Basu et al., 2001; Pettersson et al., 2000). Tumors most commonly express the 164-amino-acid isoform of VEGF-A (Nagy et al., 2003). The angiogenic response elicited upon AdVEGF-A injection in the ears of nude mice, therefore, mimicked the angiogenic response seen in tumors (Basu et al., 2001; Pettersson et al., 2000). We observed an increased angiogenic response [i.e. CD31 (also known as PECAM1) expression] in the AdVEGF-A-treated ear compared to the vehicle-treated control ear of the same mouse (Fig. 2A; P<0.005).

Interestingly, very high expression of DAD2 receptors was also observed on the ECs of angiogenic blood vessels in AdVEGF-A injected ears (Fig. 2B). In contrast, very low expression of DAD2 receptors was observed in the ECs of blood vessels in vehicle-treated control ears by confocal microscopy (Fig. 2B; P<0.05). These results, therefore, confirm the specific role of VEGF-A in regulating the expression of the DAD2 receptors on ECs.

VEGF-A induces KLF11 in endothelial cells

Along with DAD2 receptor expression, high expression of the zinc finger transcription factor Krüppel-like factor 11 (KLF11) in CD31^{+} angiogenic vessels was also observed in VEGF-A-secreting HT29 tumors (HT29+VEGF-A$^{+/+}$) compared to normal colon tissues (Fig. 3A; P<0.05). In contrast, the expression of KLF11 was significantly lower in CD31^{+} angiogenic vessels of HT29+VEGF-A$^{-/-}$ tumors (Fig. 3A; P<0.05). Similar upregulation of KLF11 was observed in the TECs of VEGF-A-secreting well-differentiated human colon adenocarcinoma tissues (Fig. 3B). In contrast, we observed very low or no expression of KLF11 in the ECs of normal colon tissues (Fig. 3B; P<0.05).

Because reports have indicated that DAD2 receptors in neuronal and endometrial cells are regulated via KLF11 (Seo et al., 2012;

Journal of Cell Science (2022) 135, jcs259617. doi:10.1242/jcs.259617

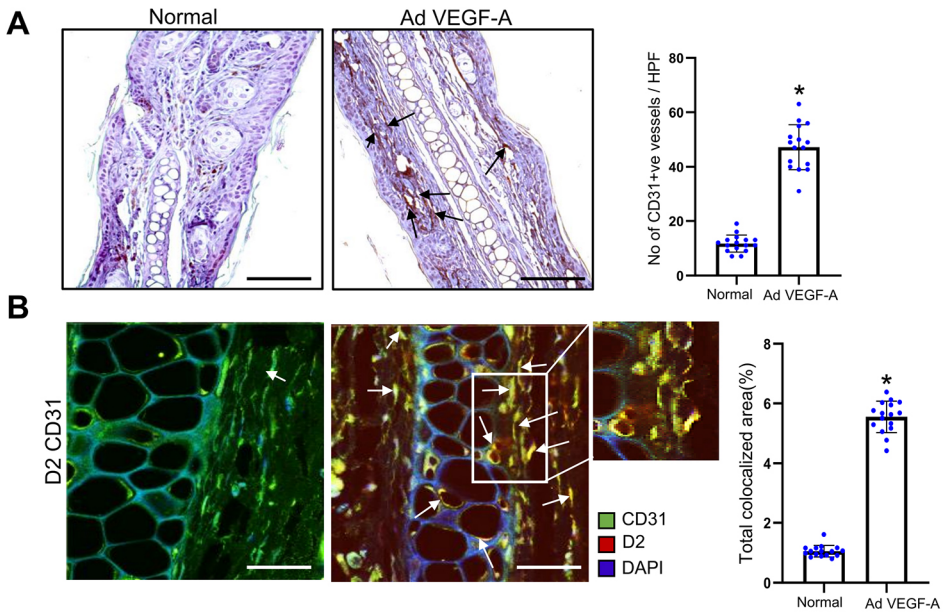

Fig. 2. High DAD2 receptor expression is observed in the endothelial cells upon AdVEGF-A injection. (A) Representative images of immunohistochemistry (arrows) showing increased angiogenesis (CD31 expression) in the AdVEGF-A-treated ear of the C57/Bl6 mouse compared to the vehicle-treated control ear of the same mouse (n=16 for each group. Scale bars: 100 µm. Right, ten randomly chosen fields were used to quantify the microvessel numbers, which is expressed as the number of microvessels/high power fields. Data are expressed as mean±s.e.m. *P<0.005 AdVEGF-A relative to vehicle-treated control (two-sample two-tailed t-test). (B) Representative images of colocalization (arrows) of CD31 and DAD2 receptors indicating higher expression of DAD2 receptors (red) on the endothelial cells (green) in AdVEGF-A-injected ears compared to endothelial cells of vehicle-treated normal ear blood vessels (n=16 for each group). Scale bars: 40 µm. Right, ten fields of view were randomly chosen and analyzed. Data are expressed as mean±s.e.m. *P<0.05 for AdVEGF-A relative to vehicle-treated control (two-sample two-tailed t-test).

Richards et al., 2017), we further investigated the effects of AdVEGF-A treatment on KLF11 expression and subsequent expression of DAD2 receptors on ECs. Accordingly, endothelial cell-specific KLF11-knockout [KLF11(−/−)] mice were developed in which KLF11 was specifically absent in the endothelial cells of these animals in comparison to the wild type controls. By contrast, KLF11 expression was evident in skeletal muscle and pancreatic tissues, as previously reported (Cook et al., 1998), thereby confirming endothelial cell-specific knockdown of KLF11 in these animals (Fig. S3A,B).

AdVEGF-A was then injected into the ears of both wild-type and endothelial cell-specific KLF11(−/−) mice. Although immunofluorescence staining showed high expression of DAD2 receptors on the ECs of ear blood vessels in wild-type animals following AdVEGF-A injection, AdVEGF-A injection into ears of endothelial cell-specific KLF11(−/−) mice failed to upregulate the expression of DAD2 receptors on ECs of ear blood vessels (Fig. 3C; P<0.05). Therefore, these data demonstrate that VEGF-A-mediated upregulation of DAD2 receptors on ECs depends upon KLF11 expression in these cells.

DA mediates inhibition of VEGF-A-stimulated tumor growth via KLF11

A major mechanism by which DA inhibits tumor growth is the suppression of VEGF-A-induced angiogenesis (Chakroborty et al., 2004; Chauvet et al., 2017; Sarkar et al., 2008; Hoeppner et al., 2015). DA acts via its D2 receptors on the TECs to inhibit VEGF-A-induced angiogenesis and thereby reduce tumor growth (Chakroborty et al., 2004; Chauvet et al., 2017; Sarkar et al., 2008; Hoeppner et al., 2015). Since our previous results indicate that VEGF-A upregulates KLF11 in ECs (Fig. 3A), which in turn stimulates DAD2 receptor expression on these cells (Fig. 3C), we subsequently performed experiments to determine the effects of treatment with DAD2 receptor agonist on the growth and angiogenesis of VEGF-A producing MC38 colon tumors grown in both normal and endothelial cell-specific KLF11(−/−) C57BL/6 mice as these tumors grow in the C57BL/6 background (Zhang et al., 2014; Hayata et al., 2013).

MC38 colon cancer cells were transplanted to wild-type and endothelial cell-specific KLF11(−/−) C57BL/6 mice. Then, treatment effects with the selective DAD2 receptor agonist quinpirole (10 mg/kg injected intraperitoneally once daily for 7 days) on MC38 tumor growth and angiogenesis in wild-type and endothelial cell-specific KLF11($^{-/-}$) mice were evaluated. The tumor inhibitory and anti-angiogenic effects of quinpirole were significantly more potent in wild type C57BL/6 mice than in endothelial cell-specific KLF11(−/−) C57BL/6 mice bearing MC38 colon tumors (Fig. 3D,E; P<0.005). These results indicate that in the absence of KLF11, the activation of DAD2 receptors on ECs by selective DAD2 receptor agonist has no significant inhibitory effect on VEGF-A-mediated MC38 colon tumor growth and angiogenesis because VEGF-A fails to upregulate the expression of DAD2 receptors on these KLF11(−/−) ECs.

VEGF-A upregulates DAD2 receptors via KLF11 through the ERK1/2 signaling pathway

We performed real-time qPCR to determine the status of KLF11 and DAD2 receptors in VEGF-A-treated cultured HUVECs. Our results indicated a gradual increase in the expressions of KLF11 and DAD2 receptors in HUVECs treated with 100 ng/ml of recombinant human VEGF-A. The increase in expression started at 1 h after treatment and was maximum at 4 h (Fig. 4A; P<0.0001). Similarly, western blot analysis also demonstrated significant upregulation of KLF11 and DAD2 receptor expressions in HUVECs treated with 100 ng/ml of recombinant human VEGF-A at 1–4 h (Fig. 4B; P<0.005). 100 ng/ml of VEGF-A was selected because the optimal

Journal of Cell Science (2022) 135, jcs259617. doi:10.1242/jcs.259617

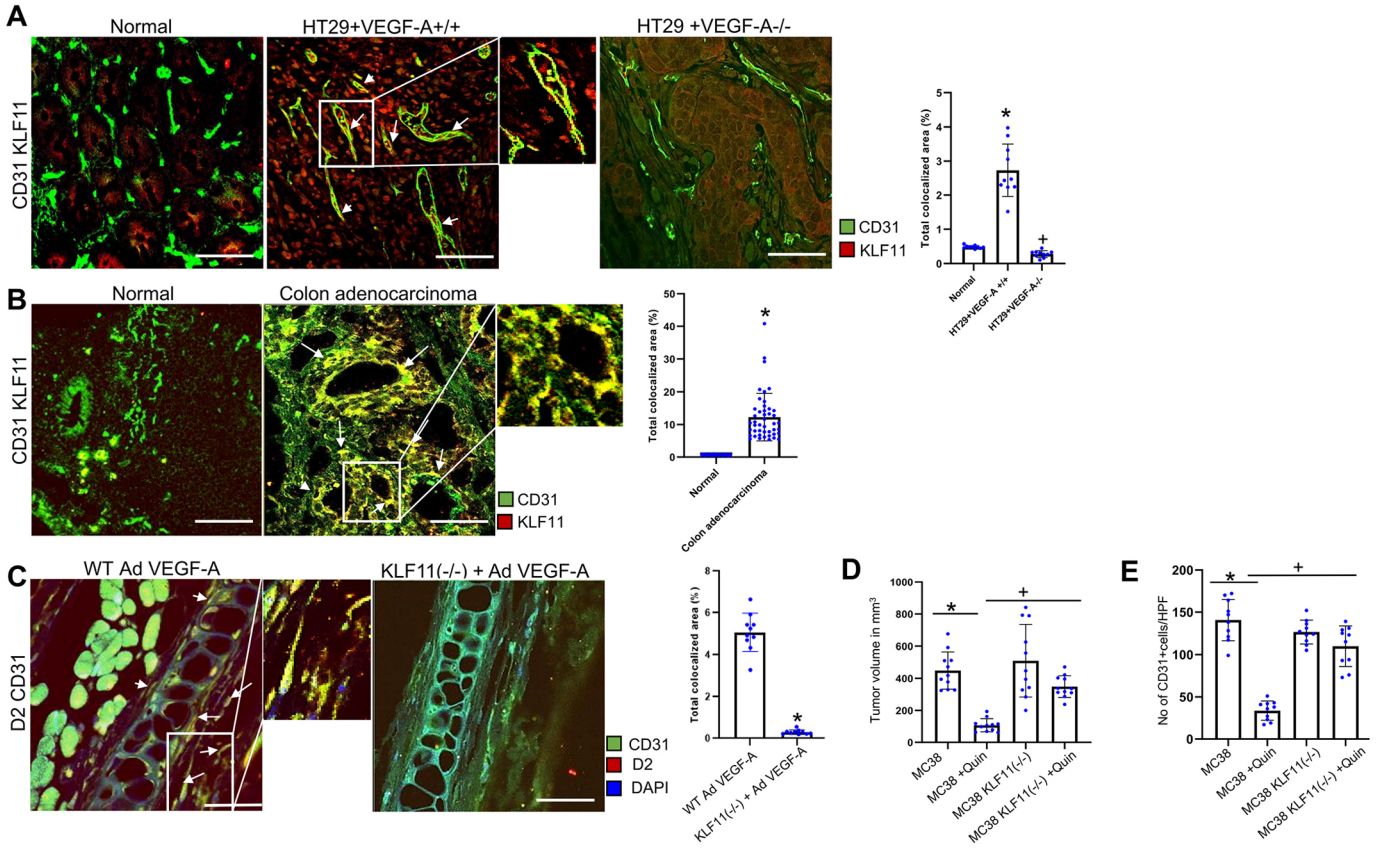

Fig. 3. VEGF-A induces KLF11 in endothelial cells. (A) Representative images of colocalization (arrows) of CD31 and KLF11 indicating significantly higher expression of KLF11 (red) in CD31-positive vessels (green) in VEGF-A-secreting HT29 tumors than CD31-positive vessels of normal colon tissues and HT29 +VEGF-A$^{-/-}$ tumors (n=10 for each group). Scale bars: 80 µm. Right, ten fields of view were randomly chosen and analyzed. Data are expressed as the mean ±s.e.m. *P<0.05 for HT29+VEGF$^{+/+}$ compared with the normal; ^{+}P<0.05 HT29+VEGF-A$^{-/-}$ compared with HT29+VEGF-A+/+ (one-way ANOVA with Bonferroni step down adjustment). (B) Representative images of colocalization (arrows) of CD31 and KLF11, indicating higher KLF11 expression (red) in tumor endothelial cells (TEC) (green) of VEGF-A-secreting well-differentiated colon adenocarcinoma tissues than on endothelial cells (green) of normal colon tissues (n=45 each group). Scale bars: 80 µm. Right, four fields of view per section were randomly chosen and analyzed. Data are expressed as the mean±s.e.m. *P<0.05 for colon adenocarcinoma compared with the normal (two-sample two-tailed t-test). (C) Colocalization (arrows) of CD31 and DAD2 receptors showing that AdVEGF-A injection into ears of wild-type (WT) C57/Bl6 mice resulted in upregulation of DAD2 receptors (red) in the endothelial cells (green) of ear blood vessels of these mice. However, AdVEGF-A injection into the ears of endothelial cell-specific KLF11(−/−) mice failed to lead to any significant upregulation in the expression of DAD2 receptors in the endothelial cells of ear blood vessels (n=10 in each group). Scale bars: 40 µm. Right, ten fields of view were randomly chosen and analyzed. Data are expressed as the mean±s.e.m. *P<0.05 for KLF11 (−/−) compared with wild-type C57/Bl6 mice injected with AdVEGF-A (two-sample two-tailed t-test). (D) DAD2 receptor agonist quinpirole (10 mg/kg of body weight intraperitoneally once daily for 7 days) significantly reduces MC38 tumor growth and (E) the number of CD31-positive cells [i.e. microvessel density (MVD) or angiogenesis]. However, inhibition by quinpirole was significantly more in tumor-bearing wild-type C57BL6 mice than in endothelial cell-specific KLF11(−/−) C57BL6 mice bearing MC38 colon tumors. Data are expressed as mean±s.e.m. *P<0.005 when compared to control MC38; +P<0.005 when compared to MC38+Quin (n=11 each group) (one-way ANOVA with Bonferroni step down adjustment). HPF, high power field of view.

angiogenic effect on ECs is observed with this concentration (Pepper et al., 1992; Xue and Greisler, 2002). However, VEGF-A induced upregulation of DAD2 receptor expression on HUVECs was abolished when ECs were subjected to KLF11 knockdown using siRNA against KLF11 (siKLF11) (50 µM) (Fig. 4C; P<0.005). The concentration of siKLF11 was optimized to ensure that it did not affect cell viability but significantly inhibited KLF11 expression.

Furthermore, when AdVEGF-A was injected into the ears of wild-type and endothelial cell-specific KLF11(−/−) mice, immunofluorescence staining indicated increased expression of KLF11 in the microvascular ECs in wild-type mice. Endothelial cell-specific KLF11(−/−) mice showed no expression of KLF11 upon AdVEGF-A injection (Fig. 5A; P<0.05).

The actions of VEGF-A are mediated through a series of downstream signaling pathways, and VEGF-A is a potent modulator of the extracellular signal-regulated kinase 1 and 2 (ERK1/2; also known as MAPK3 and MAPK1, respectively) signaling cascade that induces changes in endothelial cell behavior and regulates the subsequent process of angiogenesis (Simons et al., 2016). Accordingly, our western blot results demonstrated that VEGF-A significantly upregulated KLF11 expression in ECs. However, blocking ERK1/2 signaling by pretreating these cells with the specific ERK1/2 blocker SCH772984 (1 µM) (Bryant et al., 2019), abolished the effects of VEGF-A (Fig. 5B; P<0.005). These results show that VEGF-A can upregulate DAD2 receptors on ECs via a KLF11–ERK1/2 pathway.

DISCUSSION

Taken together, our results indicate that VEGF-A can control the expression of DAD2 receptors on ECs (Figs 1C and 2B). Furthermore, VEGF-A-mediated upregulation of DAD2 receptors on ECs is dependent on the expression of KLF11 in these cells, as this effect of VEGF-A on DAD2 receptor expression on ECs is

Journal of Cell Science (2022) 135, jcs259617. doi:10.1242/jcs.259617

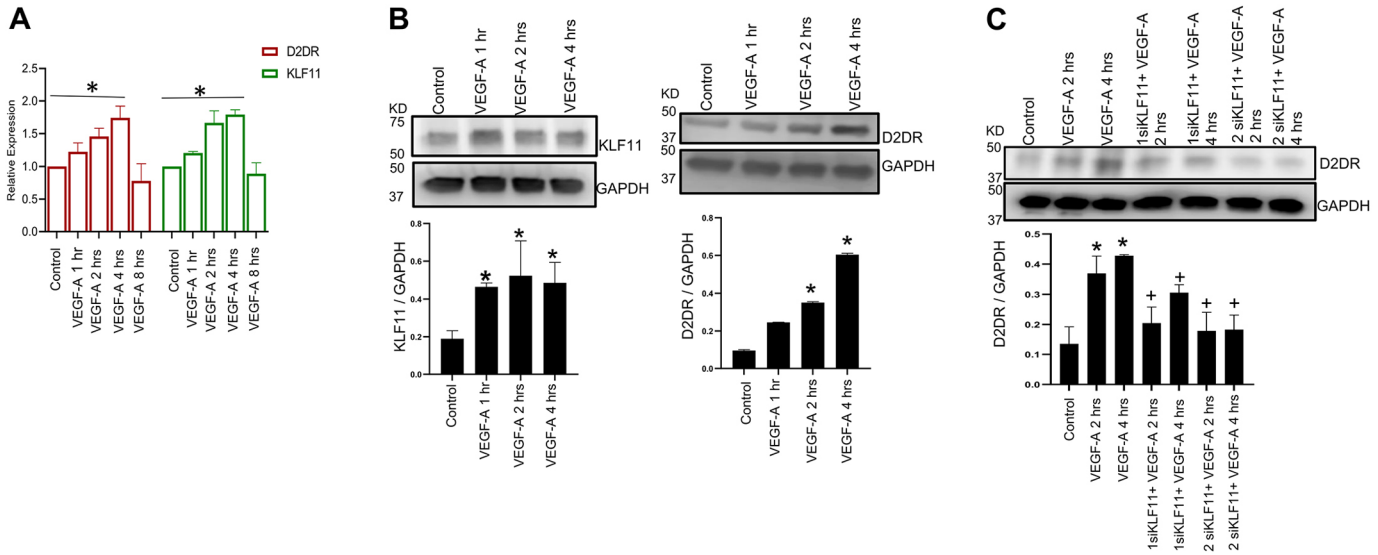

Fig. 4. KLF11 and D2DR expression in HUVECs upon treatment with VEGF-A. (A) Real-time qPCR indicates a time-dependent increase in KLF11 expression in HUVECs upon VEGF-A treatment (100 ng/ml of human recombinant VEGF-A) with maximum expression at 4 h. A similar increase was also observed in D2DR expression in HUVECs upon VEGF-A treatment. Data are expressed as mean±s.e.m., n=3 (relative to vehicle-treated control). *P<0.0001 (one-way ANOVA with Bonferroni step down adjustment). (B) Western blot analysis showing significant upregulation of KLF11 expression within 1 h of stimulation and DAD2 receptor (D2DR) expression within 2 h of stimulation in HUVECs treated with 100 ng/ml of human recombinant VEGF-A. The upregulation was also evident at 4 h. The fold changes of KLF11 and D2DR normalized to GAPDH from different experiments were averaged. Data are expressed as mean±s.e.m. and is representative of three independent experiments with similar results. *P<0.005 for VEGF-A versus vehicle control (one-way ANOVA with Bonferroni step down adjustment). (C) Western blot analysis demonstrated that VEGF-A induced upregulation of D2DR expression in HUVECs was abolished when KLF11 was knocked down in these cells by siRNA. The fold changes of D2DR normalized to GAPDH from different experiments were averaged. Data are expressed as mean±s.e.m. and is representative of three independent experiments with similar results. *P<0.005 for VEGF-A versus vehicle control; ^{+}P<0.005 for siKLF11+VEGF-A versus VEGF-A (one-way ANOVA with Bonferroni step down adjustment). KD, size in kDa.

abrogated both *in vitro* and *in vivo* when KLF11 is specifically knocked down in these cells (Figs 3C and 4C).

KLF11 is a member of the widely expressed Sp and KLF family of zinc-finger transcription factors, and these ubiquitously expressed transcription factors regulate the expression of several genes (Turner and Crossley, 1999). It has been previously reported that KLF11 can regulate the expression of DAD2 receptors in neurons and endometrial cells (Seo et al., 2012; Richards et al., 2017). Our results show that VEGF-A can induce KLF11 in ECs through the ERK1/2 pathway (Fig. 5B). This study is the first, to our knowledge, to report that VEGF-A can upregulate the expression of DAD2 receptors on ECs through the KLF11-ERK1/2 pathway (Fig. 5C).

Angiogenesis, or the formation of new blood vessels, plays a critical role in the pathogenesis of several diseases (Carmeliet, 2005). VEGF-A plays a central role in this process (Dvorak, 2005; Apte et al., 2019). We and others have previously demonstrated that DA can significantly regulate VEGF-A-induced angiogenesis by acting through its D2 receptors expressed on ECs (Basu et al., 2001; Chakroborty et al., 2004; Chauvet et al., 2017; Sarkar et al., 2008; Hoeppner et al., 2015). Interestingly, our results, for the first time, demonstrate that not only does stimulation or activation of DAD2 receptors control the actions of VEGF-A, but that VEGF-A as a feedback mechanism also regulates the expression of DAD2 receptors on ECs. VEGF-A thus acts as a potent regulator of its own proangiogenic actions. Therefore, a novel paracrine regulatory loop between VEGF-A and DAD2 receptors is observed in the tumor microenvironment, where VEGF-A secreted by tumor cells stimulates the expression of DAD2 receptors on TECs, which, on activation, inhibits the proangiogenic actions of VEGF-A. Because VEGF-A angiogenesis plays a critical role in regulating the growth and progression of tumors, including colon cancer (Garcia et al., 2020), targeting this pathway could be a therapeutic approach to inhibit tumor growth and progression and thereby influence the clinical course of the disease.

Finally, in addition to establishing a novel cytokine-mediated mechanism regulating the expression of a critical neurotransmitter/neurohormone receptor, our findings suggest the potential utility of targeting this unique link in cancer and other disorders, such as ovarian hyperstimulation syndrome and endometriosis, in which DAD2 receptors and VEGF-A-mediated angiogenesis play critical pathogenic roles in ECs (Basu et al., 2001; Chakroborty et al., 2004; Pellicer et al., 2020, 2021). Furthermore, inexpensive and selective DAD2 receptor agonists with well-established, manageable side effects are already in clinical use (Katzung, 2018). Therefore, these drugs can be tested as clinical trials in these diseases.

MATERIALS AND METHODS

Cells and reagents

HT29 cells (ATCC) and MC38 cells (a gift from Dr Mong-Heng Wang of Augusta University, Georgia, USA; Zhang et al., 2014) were cultured and maintained in McCoy's 5A medium (ATCC) supplemented with 10% fetal bovine serum (FBS) and Dulbecco's modified Eagle's medium (DMEM) (ATCC) supplemented with 10% heat-inactivated FBS, 100 mg/ml streptomycin and 100 U/ml penicillin, respectively. Human umbilical vein endothelial cells (HUVECs; Lonza, CA, USA) were cultured and maintained in endothelial cell growth medium (EGM; Lonza) supplemented with growth factors and 2% fetal calf serum (FCS; Lonza). These cell lines were recently authenticated by short tandem repeat profiling, and mycoplasma contamination was assessed via PCR (Lu et al., 2021).

Animal study

All animal procedures were approved by the IACUC of the Ohio State University. Equal numbers of male and female athymic nude (nu/nu) mice (6–8 weeks old; Charles River Laboratories) were used to establish the

Journal of Cell Science (2022) 135, jcs259617. doi:10.1242/jcs.259617

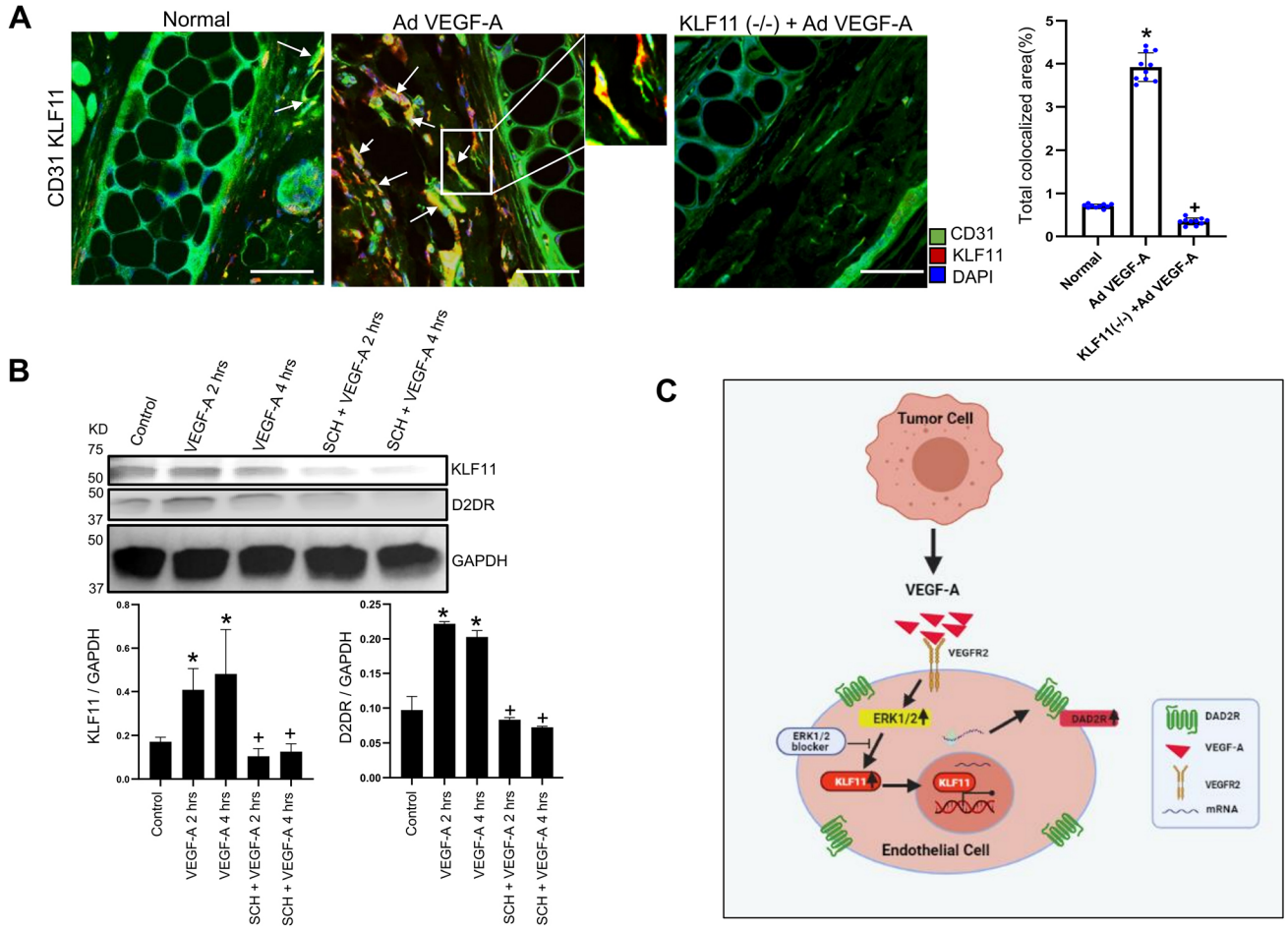

Fig. 5. VEGF-A-induced upregulation of KLF11 expression in endothelial cells is abrogated by blocking the ERK1/2 pathway. (A) AdVEGF-A injection into the ears leads to a significantly high angiogenic response (CD31) along with higher colocalization (arrows) of KLF11 (red) in the endothelial cells (CD31; green) of wild-type C57/BL6 mice but not in the endothelial cells of ear blood vessels of the endothelial cell-specific KLF11-knockout mice (n=10 for each group). Scale bars: 40 µm. Right, ten fields of view were randomly chosen and analyzed. Data are expressed as the mean±s.e.m. *P<0.05 for KLF11(−/−) injected with AdVEGF-A compared with the normal; ^{+}P<0.05 for KLF11−/− compared with wild type C57/BL6 mice, both injected with AdVEGF-A (one-way ANOVA with Bonferroni step down adjustment). (B) Western blot demonstrating that VEGF-A significantly upregulated KLF11 as well as DAD2 receptor (D2DR) expression in endothelial cells, and pretreatment of these cells with selective ERK1/2 blocker SCH772984 (SCH), 1 µM, abolished the action of VEGF-A. The fold changes of KLF11 and DAD2 receptors normalized to GAPDH from different experiments were averaged. Data are expressed as mean±s.e.m. and is representative of three independent experiments with similar results. *P<0.005 for VEGF-A versus vehicle control; ^{+}P<0.005 for SCH+VEGF-A versus VEGF-A (one-way ANOVA with Bonferroni step down adjustment). (C) A schematic diagram showing that VEGF-A secreted by tumor cells stimulates the expression of dopamine D2 receptors (DAD2R) in the endothelial cells by activating the ERK1/2 signaling cascade and upregulating KLF11 expression in these cells. This panel was created with BioRender.com.

tumor models. For the orthotopic HT29 mouse models, ketamine and xylazine [100 mg and 10 mg, respectively, intraperitoneally (i.p.)] was used to anesthetize the mice before implantation of cells (10^6 HT29 cells in 50 µl of medium) into the cecum from the serosal side through a small abdominal incision using a 30-gauge (G) needle. The cecum was replaced in the abdominal cavity, and the wound was then closed in one layer (Sarkar et al., 2008). For the MC38 colon tumor model, 1.4×10^6 MC38 colon carcinoma cells were injected subcutaneously (s.c.) (Zhang et al., 2014; Hayata et al., 2013) into the left flanks of equal numbers of 4-to 6-week-old male and female wild-type and endothelial cell-specific KLF11(−/−) C57BL/6 mice. Quinpirole (10 mg/kg of body weight, intraperitoneally once daily for 7 days, Sigma, MO) was injected into mice in the treatment groups.

Generation of VEGF-A-knockout HT29 cells

CRISPR/Cas9 gene editing was used to generate these cells (Shivram et al., 2021). In brief, gRNA plasmids (IDT, CA) PC590.VEGFA.g3 (40% cleavage activity) (5′-TTCTGCTGTCTTGGGTGCATNGG-3′) and PC590.VEGFA.g7 (32% cleavage activity) (5′-CACGACCGCTTACCTTG GCANGG-3′) were transfected together with Cas9 plasmid (IDT, CA) into HT29 cells. Puromycin (2 µg/ml, Sigma, MO) was used for cell selection. Then, single-cell cloning was performed, and cell colonies were screened by genotyping. Finally, VEGF-A-knockout clones were expanded and cryopreserved.

Development of KLF11-shRNA knock-in and endothelial-specific KLF11(−/−) mouse models

The mKLF11-shRNA knock-in (mKLF11-shRNA) mice were generated using an integrase-based approach (Tasic et al., 2011), and the reagents were from Applied StemCell, CA. The generation of the KLF11-shRNA transgenic mouse model involved four steps. The first step was to generate a genetically modified founder mouse line, designated Rosa26-3XattP (R26P3), by knocking in three tandem attP sites (3attP) into C57BL/6 (B6) mouse Rosa26 locus. KLF11 shRNA in vector pBT346 was amplified by PCR using a plasmid provided by OriGene (Worcester, MA) as a template. The second step integrated the KLF11-shRNA transgene into the R26P3 sites. This step was completed by microinjecting an integration cocktail into the pronuclei of zygotes from heterozygous R26P3 B6 mice.

The integration cocktail consisted of the plasmid pBT346-KLF11-shRNA donor vector DNA and *in vitro* transcribed ϕC31 integrase mRNA. The primers used for the generation of the knock-in mice are provided in Table S1. Finally, mice expressing mKLF11-shRNA in ECs were generated after crossing these mice with B6.Cg-Tg (Tek-cre) 1Ywa/J mice (The Jackson Laboratory, ME; Stock: 008863).

AdVEGF-A induced model of angiogenesis

Adenoviral vectors were purchased from Angio-Proteomie, MA. Adenovirus VEGF-A (AdVEGF-A) was diluted directly into PBS with 3% glycerol. Adenoviral vectors in volumes of 10 to 50 µl containing 2.5×10^5 plaque-forming units (PFU) or dilutions thereof were injected with a Hamilton syringe (10 µl) fitted with a fixed 26-G needle intradermally into the dorsal ear skin of nu/nu mice (Basu et al., 2001; Pettersson et al., 2000).

Immunofluorescence

De-identified human tissue sections were used after approval from the Ohio State University IRB. These human studies abide by the Declaration of Helsinki principles. Human normal colon and colon cancer tissues, normal mouse colon and ear tissues, HT29 colon tumor sections and KLF11(−/−) mouse ear tissues were used. Tissue sections were subjected to immunofluorescence staining to assess colocalization of CD31 (catalog no. NB100-2284, Novus Biologicals, 1:100) (Jiang et al., 2020) and KLF11 (catalog no. H00008462-M03, Abnova, 1:100) or CD31 (catalog no. NB100-2284, Novus Biologicals, 1:100) (Jiang et al., 2020) and DAD2 receptors (catalog no. sc-9113, Santa Cruz Biotechnology, 1:50) (Lu et al., 2021). Only validated and published antibodies were used (Jiang et al., 2020; Zheng et al., 2016; Lu et al., 2021). Tumor sections were pre-blocked with 10% goat serum or mouse-on-mouse blocking agent (catalog no. 2213-1, Vector Laboratories; when anti-mouse primary antibodies were used on mouse tissues) at room temperature for 1 h. Then primary antibodies were added, and the tumor sections were incubated at 4°C overnight. The sections were washed with PBS the next day, and secondary antibodies (conjugated to Alexa Fluor 488 and Alexa Fluor 633; Invitrogen) were added and incubated for 30 min at room temperature. Sections were mounted with Invitrogen ProLong Gold antifade reagent (catalog no. P10144; Thermo Fisher Scientific) for fluorescence microscopy using an Olympus FV1000 and Zeiss LSM 700 Axio Imager. Z2. Quantification of colocalized area (percentage of the total area showing colocalization) was performed by two investigators who were blind to the experimental conditions, using ImageJ software (NIH, MA, USA) and compared among groups (Chakroborty et al., 2011; Lu et al., 2021).

Immunohistochemistry

Mouse ear sections were first probed with an anti-CD31 antibody (catalog no. NB100-2284, Novus Biologicals; 1:100) overnight at 4°C and then with a secondary antibody (Vector Labs). This antibody has been validated before (Jiang et al., 2020). Images were acquired using an Axio Scope upright light microscope (Carl Zeiss, Oberkochen). Microvessel density was determined by assessing CD31 staining, a well-established marker of angiogenesis, in ten random microscopic fields using ImageJ software (NIH, MA, USA). Quantitative analysis was performed by two investigators who were blind to the experimental conditions, as described previously (Chakroborty et al., 2008; Lu et al., 2021).

Real-time qPCR

Total RNA was isolated from HT29+VEGF-A+/+, HT29+VEGF-A−/− cells and VEGF-A-treated (100 ng/ml for 1, 2, 4, 8 h) HUVECs using the RNeasy Mini Kit (Qiagen) according to the manufacturer's protocol. RNA concentration was determined by using a NanoDrop spectrophotometer (Thermo Fisher Scientific). cDNA synthesis was carried out using the RevertAid™ premium first-strand cDNA synthesis system by Thermo Fisher Scientific for RT-PCR using oligo(dT) primers. Real-time PCR was performed with SYBER green mixed (catalog no. K0221, Thermo Fisher Scientific) using the QuantStudio™ 3 Real-Time PCR System (Applied Biosystem, MA) in 96-well format, to confirm the expression of VEGFA, KLF11 and DAD2 receptor in the samples using first-strand cDNA as templates. Real-time PCR primers were designed for genes using gene sequences from the GenBank database. The expression of GAPDH served as an endogenous control. Final data were expressed in arbitrary units (relative expression), and the fold change in gene expression was determined using the ΔΔCt method. Real-time PCR for each gene was performed in triplicate (Schmittgen and Livak, 2008). Primers used were: VEGFA (forward, 5′-TTGCCTTGCTGCTCTACCTCCA-3′; reverse, 5′-GATGGC-AGTAGCTGCGCTGATA-3′), KLF11 (forward, 5′-ATGGATGCAGCCA-CACCTGAAC-3′; reverse, 5′-GGAGAAACAGGTGTCCTTGTCG-3′), DAD2 receptor (forward, 5′-CAATACGCGCTACAGCTCCAAG; reverse, 5′-GGCAATGATGCACTCGTTCTGG), GAPDH (forward, 5′-GTCTCC-TCTGACTTCAACAGCG; reverse, 5′-ACCACCCTGTTGCTGTAGCCA-A-3′) (Invitrogen).

ELISA

HT29+VEGF-A$^{+/+}$ and HT29+VEGF-A$^{-/-}$ cells were maintained in culture for 48 h, and the media were collected. The ELISA assay for VEGF-A determination was performed using a Quantikine ELISA Kit (R&D Systems, Minneapolis, MN), and absorbance was measured at 450 nm using a PowerWave XS Microplate reader (BioTek Instruments, VT) (Chakroborty et al., 2016).

Western blotting

Western blot analyses were performed on HUVECs using antibodies against KLF11 (catalog no. TA811001, Origene, 1:1000) (Sun et al., 2021), GAPDH (catalog no. 2118, Cell Signaling Technology, 1:1000) (Ren et al., 2021), DAD2 receptor (catalog no. sc-5303, Santa Cruz Biotechnology, 1:200) (Morales-Mulia et al., 2020) and phospho- and total ERK1/2 (catalog nos 9101 and 4695 Cell Signaling Technology, 1:1000) (Yoon et al., 2021). Only validated and published antibodies were used (Sun et al., 2021; Ren et al., 2021; Morales-Mulia et al., 2020; Yoon et al., 2021). An equal amount of protein (40 µg of cell lysates) was electrophoresed on a polyacrylamide gel. Proteins were transferred to 0.2 µm PVDF membranes using a Bio-Rad Trans-Blot TurboTM Transfer Pack. Membranes were pre-blocked with either 5% bovine serum albumin (BSA; for detection of phosphoproteins) or nonfat dried milk in Tris-buffered saline (TBS; 5%) and then incubated with primary and horseradish peroxidase (HRP)-conjugated secondary antibodies. Molecular masses of protein bands were determined by using a protein molecular mass marker (Precision Plus protein Standards, Bio-Rad) that was run on the same gel. C-Digit blot scanner (LI-COR, NE) was used to obtain band images. Representative bands were measured by densitometry (ImageJ NIH) and compared between the groups. GAPDH was used as an internal control. Then to detect GAPDH, the same blots were incubated with stripping buffer (catalog number: PB-96 –Strong, Boston BioProducts) for 45 min at 60°C, washed thoroughly in PBST, and blocked again in TBS with 5% dried milk before reprobing for GAPDH overnight (Chakroborty et al., 2011; Lu et al., 2021). SCH772984 (a specific ERK1/2 inhibitor) was from Selleckchem, TX, USA (catalog no. S7101). Original uncropped images of western blots are shown in Fig. S4.

siRNA knockdown of KLF11 in HUVECs

siRNA targeting KLF11 (ON-TARGETplus Human KLF11 (8462) siRNA, catalog number: LQ-006598-00-0002; J-006598-05-0002 and J-006598-06-0002) was purchased from Horizon Discovery Biosciences (Dharmacon) and diluted using serum-free medium containing transfection reagents. HUVECs were plated 1 day before transfection in 12-well plates. Upon reaching 60–70% confluence, HUVECs were transfected with siKLF11 and negative universal control Silencer™ Negative Control No. 1 siRNA [catalog no. D-001810-10-05, Horizon Discovery Biosciences (Dharmacon)] by magnetofection using SilenceMag beads (OZ Biosciences, CA) (Dou et al., 2015). siRNA concentration was optimized to ensure that cell viability was not affected. Knockdown of KLF11 in HUVECs was confirmed after post-transfection by western blot analysis, and siKLF11-transfected HUVECs were used to assess the effect of VEGF-A on the expression of DAD2 receptors.

Statistical analysis

All data are expressed as the mean±s.e.m. Differences between independent groups were evaluated by one-way ANOVA with Bonferroni step down

adjustment for experiments involving more than two groups and by a two-sample *t*-test for experiments with two groups. A paired two-tailed *t*-test was used to compare differences between treated and untreated mouse ears. *P*-values of multiple comparisons were adjusted by the Bonferroni method. $P<0.05$ was considered significant (Basu et al., 2001; Yang et al., 2019).

Acknowledgements
The authors acknowledge the use of confocal microscopes at the Microscopy Shared Resources (Comprehensive Cancer Center) and Pathology core facility of the Ohio State University. C.S and D.C. were also supported by funding from Mitchell Cancer Institute, University of South Alabama,Mobile, Alabama, USA.

Competing interests
The authors declare no competing or financial interests.

Author contributions
Conceptualization: S.B.; Methodology: C.S., D.C., S.G., S.B.; Validation: C.S., D.C., S.G., H.F., S.B.; Formal analysis: C.S., D.C., S.G., X.M., S.B.; Investigation: C.S., D.C., S.G., H.F.; Resources: S.B.; Data curation: C.S., D.C., S.G., S.B.; Writing - original draft: C.S., D.C., S.G., S.B.; Writing - review & editing: C.S., D.C., S.G., X.M., S.B.; Visualization: C.S., D.C., S.G., S.B.; Supervision: S.B.; Project administration: S.B.; Funding acquisition: C.S., D.C., S.B.

Funding
This study was supported by the National Institutes of Health (NIH)/NCI, USA (R01 CA169158); NIH/NHLBI, USA (R01 HL131405 to S.B.); Department of Defense, USA (W81XWH-19-1-0233 and W81XWH2110874 to S.B.); C.S. was partially supported by NIH/NCI, USA (R21 CA216763 to C.S.); D.C. was partially supported by Department of Defense USA (W81XWH-20-1-0618 to D.C.). Deposited in PMC for release after 12 months.

References
Apte, R. S., Chen, D. S. and Ferrara, N. (2019). VEGF in signaling and disease: beyond discovery and development. *Cell* **176**, 1248-1264. doi:10.1016/j.cell.2019.01.021

Basu, S., Nagy, J. A., Pal, S., Vasile, E., Eckelhoefer, I. A., Bliss, V. S., Manseau, E. J., Dasgupta, P. S., Dvorak, H. F. and Mukhopadhyay, D. (2001). The neurotransmitter dopamine inhibits angiogenesis induced by vascular permeability factor/vascular endothelial growth factor. *Nat. Med.* **7**, 569-574. doi:10.1038/87895

Basu, S., Sarkar, C., Chakroborty, D., Nagy, J., Mitra, R. B., Dasgupta, P. S. and Mukhopadhyay, D. (2004). Ablation of peripheral dopaminergic nerves stimulates malignant tumor growth by inducing vascular permeability factor/vascular endothelial growth factor-mediated angiogenesis. *Cancer Res.* **64**, 5551-5555. doi:10.1158/0008-5472.CAN-04-1600

Beaulieu, J.-M., Espinoza, S. and Gainetdinov, R. R. (2015). Dopamine receptors - IUPHAR Review 13. *Br. J. Pharmacol.* **172**, 1-23. doi:10.1111/bph.12906

Bryant, K. L., Stalnecker, C. A., Zeitouni, D., Klomp, J. E., Peng, S., Tikunov, A. P., Gunda, V., Pierobon, M., Waters, A. M., George, S. D. et al. (2019). Combination of ERK and autophagy inhibition as a treatment approach for pancreatic cancer. *Nat. Med.* **25**, 628-640. doi:10.1038/s41591-019-0368-8

Carmeliet, P. (2005). Angiogenesis in life, disease and medicine. *Nature* **438**, 932-936. doi:10.1038/nature04478

Chakroborty, D., Sarkar, C., Mitra, R. B., Banerjee, S., Dasgupta, P. S. and Basu, S. (2004). Depleted dopamine in gastric cancer tissues: dopamine treatment retards growth of gastric cancer by inhibiting angiogenesis. *Clin. Cancer. Res.* **10**, 4349-4356. doi:10.1158/1078-0432.CCR-04-0059

Chakroborty, D., Chowdhury, U. R., Sarkar, C., Baral, R., Dasgupta, P. S. and Basu, S. (2008). Dopamine regulates endothelial progenitor cell mobilization from mouse bone marrow in tumor vascularization. *J. Clin. Invest.* **118**, 1380-1389. doi:10.1172/JCI33125

Chakroborty, D., Sarkar, C., Yu, H., Wang, J., Liu, Z., Dasgupta, P. S. and Basu, S. (2011). Dopamine stabilizes tumor blood vessels by up-regulating angiopoietin 1 expression in pericytes and Krüppel-like factor-2 expression in tumor endothelial cells. *Proc. Natl. Acad. Sci. USA* **108**, 20730-20735. doi:10.1073/pnas.1108696108

Chakroborty, D., Sarkar, C., Lu, K., Bhat, M., Dasgupta, P. S. and Basu, S. (2016). Activation of dopamine D1 receptors in dermal fibroblasts restores vascular endothelial growth factor-a production by these cells and subsequent angiogenesis in diabetic cutaneous wound tissues. *Am. J. Pathol.* **186**, 2262-2270. doi:10.1016/j.ajpath.2016.05.008

Chauvet, N., Romanò, N., Lafont, C., Guillou, A., Galibert, E., Bonnefont, X., Le Tissier, P., Fedele, M., Fusco, A., Mollard, P. et al. (2017). Complementary actions of dopamine D2 receptor agonist and anti-vegf therapy on tumoral vessel normalization in a transgenic mouse model. *Int. J. Cancer* **140**, 2150-2161. doi:10.1002/ijc.30628

Cook, T., Gebelein, B., Mesa, K., Mladek, A. and Urrutia, R. (1998). Molecular cloning and characterization of *TIEG2* reveals a new subfamily of transforming growth factor-β-inducible Sp1-like zinc finger-encoding genes involved in the regulation of cell growth. *J. Biol. Chem.* **273**, 25929-25936. doi:10.1074/jbc.273.40.25929

Dou, L., Sallée, M., Cerini, C., Poitevin, S., Gondouin, B., Jourde-Chiche, N., Fallague, K., Brunet, P., Calaf, R., Dussol, B. et al. (2015). The cardiovascular effect of the uremic solute indole-3 acetic acid. *J. Am. Soc. Nephrol.* **26**, 876-887. doi:10.1681/ASN.2013121283

Dvorak, H. F. (2005). Angiogenesis: update 2005. *J. Thromb. Haemost.* **3**, 1835-1842. doi:10.1111/j.1538-7836.2005.01361.x

Folkman, J. (2004). Endogenous angiogenesis inhibitors. *APMIS* **112**, 496-507. doi:10.1111/j.1600-0463.2004.apm11207-0809.x

Franco, R., Reyes-Resina, I. and Navarro, G. (2021). Dopamine in health and disease: much more than a Neurotransmitter. *Biomedicines* **9**, 109. doi:10.3390/biomedicines9020109

Garcia, J., Hurwitz, H. I., Sandler, A. B., Miles, D., Coleman, R. L., Deurloo, R. and Chinot, O. L. (2020). Bevacizumab (Avastin®) in cancer treatment: A review of 15 years of clinical experience and future outlook. *Cancer Treat. Rev.* **86**, 102017. doi:10.1016/j.ctrv.2020.102017

Hayata, K., Iwahashi, M., Ojima, T., Katsuda, M., Iida, T., Nakamori, M., Ueda, K., Nakamura, M., Miyazawa, M., Tsuji, T. et al. (2013). Inhibition of IL-17A in tumor microenvironment augments cytotoxicity of tumor-infiltrating lymphocytes in tumor-bearing mice. *PLoS ONE* **8**, e53131. doi:10.1371/journal.pone.0053131

Hoeppner, L. H., Wang, Y., Sharma, A., Javeed, N., Van Keulen, V. P., Wang, E., Yang, P., Roden, A. C., Peikert, T., Molina, J. R. et al. (2015). Dopamine D2 receptor agonists inhibit lung cancer progression by reducing angiogenesis and tumor infiltrating myeloid derived suppressor cells. *Mol. Oncol.* **9**, 270-281. doi:10.1016/j.molonc.2014.08.008

Jayson, G. C., Hicklin, D. J. and Ellis, L. M. (2012). Anti-angiogenic therapy–evolving view based on clinical trial results. *Nat. Rev. Clin. Oncol.* **9**, 297-303. doi:10.1038/nrclinonc.2012.8

Jiang, D., Christ, S., Correa-Gallegos, D., Ramesh, P., Gopal, S. K., Wannemacher, J., Mayr, C. H., Lupperger, V., Yu, Q., Ye, H. et al. (2020). Injury triggers fascia fibroblast collective cell migration to drive scar formation through N-cadherin. *Nat. Commun.* **11**, 5653. doi:10.1038/s41467-020-19425-1

Katzung, B. (2018). *Basic and Clinical Pharmacology*, 14th edn. New York: McGraw Hill Education Lange.

Lu, K., Bhat, M., Peters, S., Mitra, R., Mo, X., Oberyszyn, T. M., Dasgupta, P. S. and Basu, S. (2021). Dopamine prevents ultraviolet B-induced development and progression of premalignant cutaneous lesions through its D_2 receptors. *Cancer Prev. Res. (Phila).* **14**, 687-696. doi:10.1158/1940-6207.CAPR-21-0052

Missale, C., Nash, S. R., Robinson, S. W. and Caron, M. G. (1998). Dopamine receptors: from structure to function. *Physiol. Rev.* **78**, 189-225. doi:10.1152/physrev.1998.78.1.189

Morales-Mulia, S., Magdaleno-Madrigal, V. M., Nicolini, H., Genis-Mendoza, A. and Morales-Mulia, M. (2020). Orexin-A upregulates dopamine D2 receptor and mRNA in the nucleus accumbens Shell. *Mol. Biol. Rep.* **47**, 9689-9697. doi:10.1007/s11033-020-05979-2

Nagy, J. A., Dvorak, A. M. and Dvorak, H. F. (2003). VEGF-A (164/165) and PIGF: roles in angiogenesis and arteriogenesis. *Trends Cardiovasc. Med.* **13**, 169-175. doi:10.1016/S1050-1738(03)00056-2

Pellicer, N., Galliano, D. and Pellicer, A. (2020). Ovarian Hyperstimulation Syndrome. In *The Ovary*, 3rd edn. (ed. P. Leung and E. Adashi), pp. 345-361. Cambridge, MA: Academic Press.

Pellicer, N., Galliano, D., Herraiz, S., Bagger, Y. Z., Arce, J.-C. and Pellicer, A. (2021). Use of dopamine agonists to target angiogenesis in women with endometriosis. *Hum. Reprod.* **36**, 850-858. doi:10.1093/humrep/deaa337

Pepper, M. S., Ferrara, N., Orci, L. and Montesano, R. (1992). Potent synergism between vascular endothelial growth factor and basic fibroblast growth factor in the induction of angiogenesis in vitro. *Biochem. Biophys. Res. Commun.* **189**, 824-831. doi:10.1016/0006-291X(92)92277-5

Pettersson, A., Nagy, J. A., Brown, L. F., Sundberg, C., Morgan, E., Jungles, S., Carter, R., Krieger, J. E., Manseau, E. J., Harvey, V. S. et al. (2000). Heterogeneity of the angiogenic response induced in different normal adult tissues by vascular permeability factor/vascular endothelial growth factor. *Lab. Invest.* **80**, 99-115. doi:10.1038/labinvest.3780013

Ren, J., Xu, Y., Lu, X., Wang, L., Ide, S., Hall, G., Souma, T., Privratsky, J. R., Spurney, R. F. and Crowley, S. D. (2021). Twist1 in podocytes ameliorates podocyte injury and proteinuria by limiting CCL2-dependent macrophage infiltration. *JCI Insight* **6**, e148109. doi:10.1172/jci.insight.148109

Richards, E. G., Zheng, Y., Shenoy, C. C., Ainsworth, A. J., Delaney, A. A., Jones, T. L., Khan, Z. and Daftary, G. S. (2017). KLF11 is an epigenetic mediator of DRD2/dopaminergic signaling in endometriosis. *Reprod. Sci.* **24**, 1129-1138. doi:10.1177/1933719117698582

Rubí, B. and Maechler, P. (2010). Minireview: new roles for peripheral dopamine on metabolic control and tumor growth: let's seek the balance. *Endocrinology* **151**, 5570-5581. doi:10.1210/en.2010-0745

Sarkar, C., Chakroborty, D., Chowdhury, U. R., Dasgupta, P. S. and Basu, S. (2008). Dopamine increases the efficacy of anticancer drugs in breast and colon

cancer preclinical models. *Clin. Cancer. Res.* **14**, 2502-2510. doi:10.1158/1078-0432.CCR-07-1778

Schmittgen, T. D. and Livak, K. J. (2008). Analyzing real-time PCR data by the comparative C(T) method. *Nat. Protoc.* **3**, 1101-1108. doi:10.1038/nprot.2008.73

Seo, S., Lomberk, G., Mathison, A., Buttar, N., Podratz, J., Calvo, E., Iovanna, J., Brimijoin, S., Windebank, A. and Urrutia, R. (2012). Krüppel-like factor 11 differentially couples to histone acetyltransferase and histone methyltransferase chromatin remodeling pathways to transcriptionally regulate dopamine D2 receptor in neuronal cells. *J. Biol. Chem.* **287**, 12723-12735. doi:10.1074/jbc.M112.351395

Shivram, H., Cress, B. F., Knott, G. J. and Doudna, J. A. (2021). Controlling and enhancing CRISPR systems. *Nat. Chem. Biol.* **17**, 10-19. doi:10.1038/s41589-020-00700-7

Simons, M., Gordon, E. and Claesson-Welsh, L. (2016). Mechanisms and regulation of endothelial VEGF receptor signalling. *Nat. Rev. Mol. Cell. Biol.* **17**, 611-625. doi:10.1038/nrm.2016.87

Sun, Y., Qu, J., Wang, J., Zhao, R., Wang, C., Chen, L. and Hou, X. (2021). Clinical and functional characteristics of a novel *KLF11* Cys354Phe variant involved in maturity-onset diabetes of the young. *J. Diabetes Res* **2021**, 7136869. doi:10.1155/2021/7136869

Tasic, B., Hippenmeyer, S., Wang, C., Gamboa, M., Zong, H., Chen-Tsai, Y. and Luo, L. (2011). Site-specific integrase-mediated transgenesis in mice via pronuclear injection. *Proc. Natl. Acad. Sci. USA* **108**, 7902-7907. doi:10.1073/pnas.1019507108

Tejada, M. Á., Santos-Llamas, A. I., Fernández-Ramírez, M. J., Tarín, J. J., Cano, A. and Gómez, R. (2021). A reassessment of the therapeutic potential of a dopamine receptor 2 agonist (D2-AG) in endometriosis by comparison against a standardized antiangiogenic treatment. *Biomedicines* **9**, 269. doi:10.3390/biomedicines9030269

Turner, J. and Crossley, M. (1999). Mammalian Krüppel-like transcription factors: more than just a pretty finger. *Trends Biochem. Sci.* **24**, 236-240. doi:10.1016/S0968-0004(99)01406-1

Xue, L. and Greisler, H. P. (2002). Angiogenic effect of fibroblast growth factor-1 and vascular endothelial growth factor and their synergism in a novel in vitro quantitative fibrin-based 3-dimensional angiogenesis system. *Surgery* **132**, 259-267. doi:10.1067/msy.2002.125720

Yang, H., Yang, J., Cheng, H., Cao, H., Tang, S., Wang, Q., Zhao, J., Li, B., Ding, Y. and Ma, C. (2019). Probiotics ingestion prevents HDAC11-induced DEC205+ dendritic cell dysfunction in night shift nurses. *Sci. Rep.* **9**, 18002. doi:10.1038/s41598-019-54558-4

Yoon, C., Lu, J., Ryeom, S. W., Simon, M. C. and Yoon, S. S. (2021). PIK3R3, part of the regulatory domain of PI3K, is upregulated in sarcoma stem-like cells and promotes invasion, migration, and chemotherapy resistance. *Cell Death Dis.* **12**, 749. doi:10.1038/s41419-021-04036-5

Zhang, Y., Hoda, M. N., Zheng, X., Li, W., Luo, P., Maddipati, K. R., Seki, T., Ergul, A. and Wang, M.-H. (2014). Combined therapy with COX-2 inhibitor and 20-HETE inhibitor reduces colon tumor growth and the adverse effects of ischemic stroke associated with COX-2 inhibition. *Am. J. Physiol. Regul. Integr. Comp. Physiol.* **307**, R693-R703. doi:10.1152/ajpregu.00422.2013

Zheng, Y., Khan, Z., Zanfagnin, V., Correa, L. F., Delaney, A. A. and Daftary, G. S. (2016). Epigenetic modulation of collagen 1A1: therapeutic implications in fibrosis and endometriosis. *Biol. Reprod.* **94**, 87. doi:10.1095/biolreprod.115.138115

GAAGCCGGGCTCATGGACGGGTGAGGCGGCGGTGTGCGCAGACAGTGCTCCAGCCGCGCGCGCTCCCCAGGCCC
TGGCCCGGGCCTCGGGCCGGGGAGGAAGAGTAGCTCGCCGAGGCGCCGAGGAGAGCGGGCCGCCCCACAGCCC
GAGCCGGAGAGGGAGCGCGAGCCGCGCCGGCCCCGGTCGGGCCTCCGAAACCATGAACTTTCTGCTGTCTTGGG
TG↓CATTGGAGCCTTGCCTTGCTGCTCTACCTCCACCATGC↓CAAGGTAAGCGGTCGTGCCCTGCTGGCGCCGCG
GGCCGCTGCGAGCGCCTCTCCCGGCTGGGGACGTGCGTGCGAGCGCGCGCGTGGGGGCTCCGTGCCCCACGCGG
GTCCATGGGCACCAGGCGTGCGGCGTCCCCCTCTGTCGTCTTAGG

Fig. S1. PCR sequence (wild type) and the cutting edge used for the knockdown of VEGF-A in HT29 cells . PCR primers; hVEGF-A exon 1; start codon; gRNA g3; gRNA g7; ↓ gRNA cutting site.

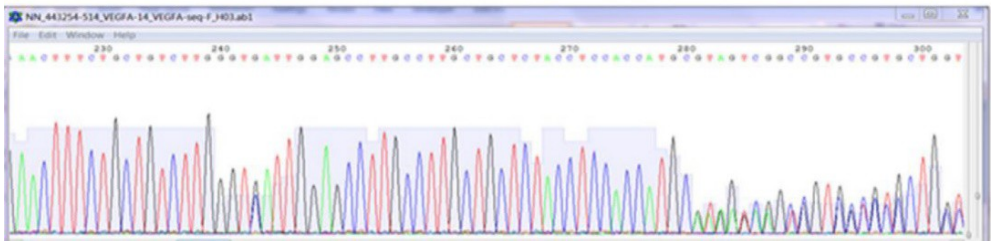

Fig. S2. PCR genotyping data of HT29 hVEGF-A ($^{-/-}$) human colon cancer cell line clone.

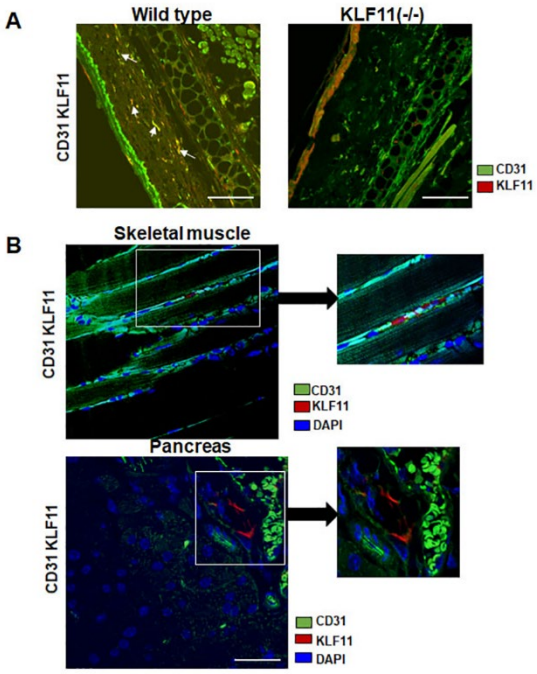

Fig. S3 (A and B). (A) Confocal images (arrows) show colocalization of KLF11 and CD31, i.e., expression of KLF11 in the endothelial cells of ears in wild type (KLF11 ($^{+}/^{+}$) C57/Bl6 mice. In contrast, there are no expressions of KLF11 in endothelial cells of ears in KLF11 ($^{-}/^{-}$) C57/Bl6 mice (Scale Bar 40 µm). (B) KLF11 expression is specifically absent in CD31 positive endothelial cells in KLF11 expressing skeletal muscle and pancreas collected from endothelial cell-specific KLF11 ($^{-}/^{-}$) mice (Scale Bar 40 µm).

Fig S4. Blot transparency.

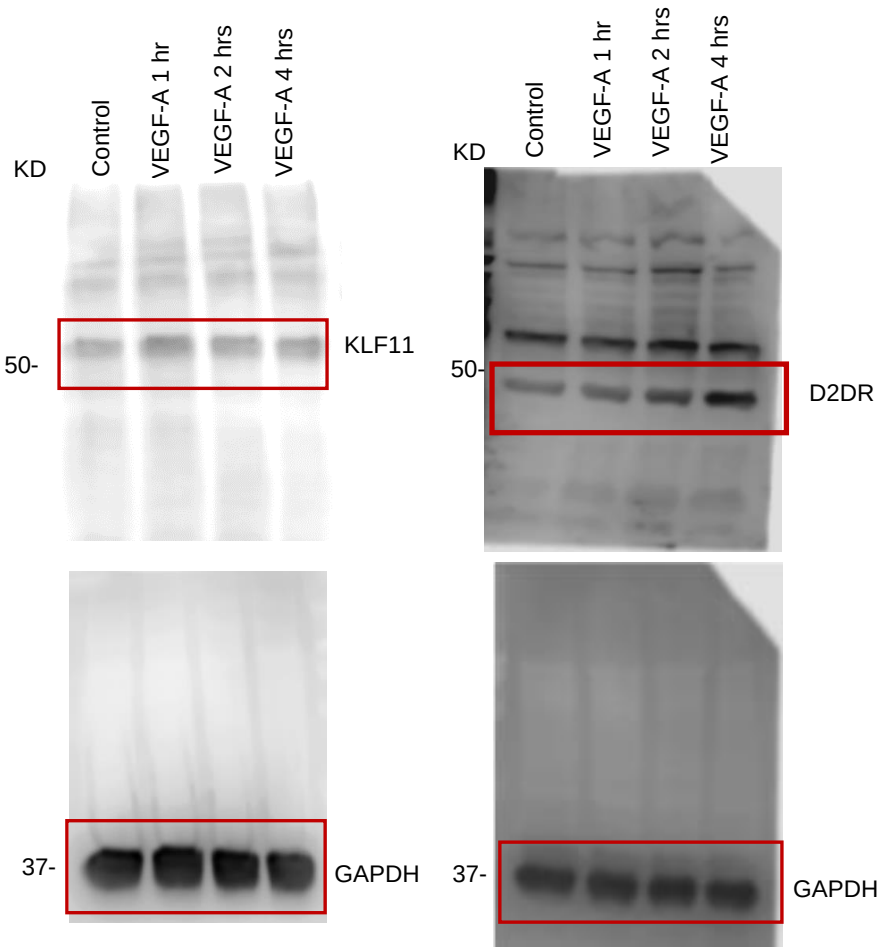

Full unedited gels for Figure 4B

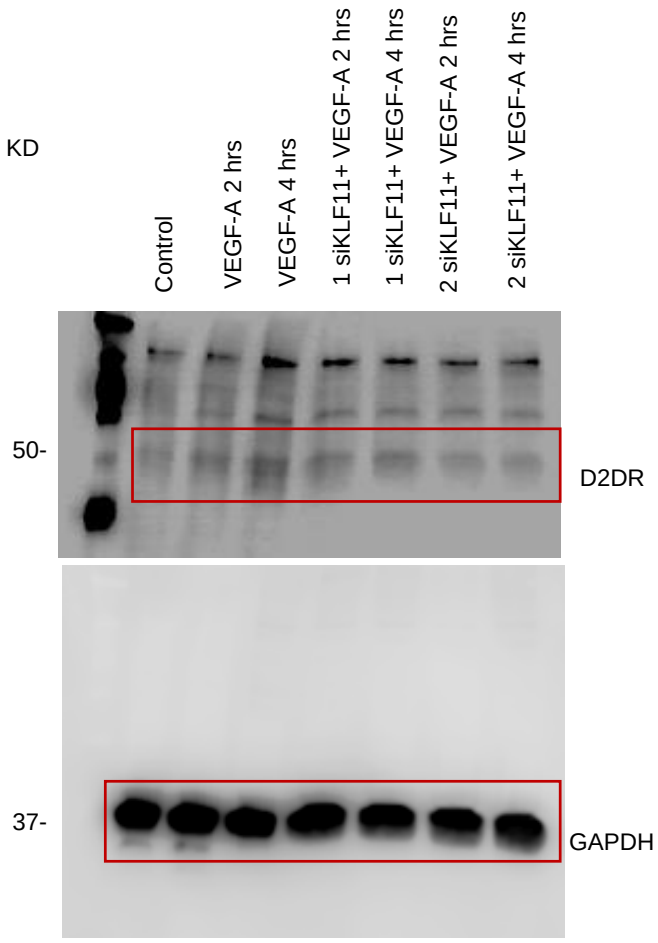

Full unedited gels for Figure 4C

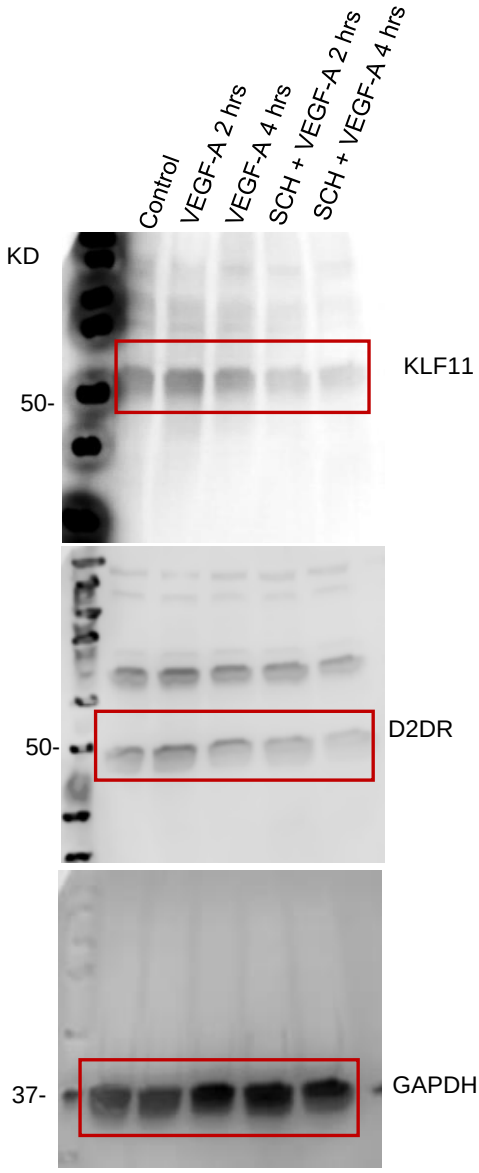

Full unedited gels for Figure 5B

Table S1. Primers used for generation of the KLF11 shRNA knockin mice

Primers	Sequence
PR425N	5′- GGTGATAGGTGGCAAGTGGTATTCCGTAAG -3′
PR436N-1	5′- ATCAACTACCGCCACCTCGACC -3′
KLF-R1	5′- CTACTTCCATTTGTCACGTCCTGCACG -3′
KLF-R2	5′- CTAGAGCGGCCGATGAGTT -3′
KLF STOP5-F	5′- GAAGCGGGTAGGCCTTTGG -3′
KLF STOP5-R	5′- TAGCCGAATAGCCTCTCCACC -3′
KLF-F	5′- GACAGCACAAAAGGAAACTCACCCTAAC -3′
PR522N	5′- GACGATGTAGGTCACGGTCTCGAAG -3′
Frt-R1	5′- GGAATAGGAACTTCGTCGACA -3′
Frt-R2	5′- CCGCGAAGTTCCTATACCTTTTG -3′
R10N	5′- AGTTCTCTGCTGCCTCCTGGCTTCT -3′
R13	5′- CATAAACCCCAGATGACTCCTATCCTC-3′